Int J Earth Sci (Geol Rundsch) (2016) 105:1729–1740
DOI 10.1007/s00531-015-1162-6

ORIGINAL PAPER

Fault kinematics and stress fields in the Rwenzori Mountains, Uganda

Till Sachau[1] · Daniel Koehn[2] · D. Sarah Stamps[3,4] · Michael Lindenfeld[5]

Received: 11 November 2013 / Accepted: 5 March 2015 / Published online: 18 March 2015

Abstract The Rwenzori Mountains in western Uganda form an active rift-transfer zone in the western branch of the East African Rift System. Here we quantify local stress fields in high resolution from field observations of fault structures to shed light on the complex, polyphase tectonics expected in transfer zones. We apply the multiple inverse method, which is optimized for heterogeneous fault-slip data, to the northern and central Rwenzori Mountains. Observations from the northern Rwenzori Mountains show larger heterogeneity than data from the central Rwenzori, including unexpected compressional features; thus the local stress field indicates polyphase transpressional tectonics. We suggest that transpression here is linked to rotational and translational movements of the neighboring Victoria block relative to the Rwenzori block that includes strong overprinting relationships. Stress inversions of data from the central Rwenzori Mountains indicate two distinct local stress fields. These results suggest that the Rwenzori block consists of smaller blocks.

✉ Till Sachau
till.sachau@gmail.com

[1] Department of Geosciences, Eberhard Karls University, Tübingen, Germany

[2] School of Geographical & Earth Sciences, University of Glasgow, Glasgow, UK

[3] Department of Earth, Atmospheric, and Planetary Sciences, Massachusetts Institute of Technology, 77 Massachusetts Ave., Cambridge, MA 02139, USA

[4] Present Address: Department of Earth, Planetary and Space Sciences, University of California, 595 Charles Young Drive East, Los Angeles, CA 90095, USA

[5] Institut für Geowissenschaften, Goethe-Universität Frankfurt, Frankfurt, Germany

Keywords Rwenzori · East African Rift System · Stress field · Stress inversion · Tectonics · Kinematics

Introduction

The Rwenzori Mountains are the highest non-volcanic mountains in Africa, located in a rift-transfer zone within the northern western branch of the East African Rift System (EARS) (Figs. 1, 2). Figure 1 gives an overview of the location of the study area and its relation to EARS. The East African Rift System is composed of the eastern and the western branches, which define the Victoria plate, roughly identical to the Tanzania craton (Calais et al. 2006).

Rift-transfer zones caused by along-strike segmentation are common features of continental rift systems (e.g., Bosworth 1985; Morley and Nelson 1990; Foster and Francis 1996), usually leading to en echelon stepping of laterally continuous rift segments. Stress fields related to these structures are complex and can yield valuable insight into the major and minor forces acting in the region (Delvaux and Barth 2010). Geological structures that develop in active rift-transfer zones include rift basin inversions, reverse faulting in a region with a dominant tensile regime, and polyphase fault/slip (Macdonald et al. 1991; Moustafa 1997; Shan et al. 2004). These structures cannot be explained by a singular uniform stress field.

Advancing our knowledge of local stress fields associated with rift-transfer zones will provide constraints on local kinematics that are needed to understand the dynamics and the relevant factors for their tectonic evolution. Here, we present new, high-resolution fault-slip data from the Rwenzori area and perform stress inversion calculations with these data sets. Local data sets were collected in small, clearly defined areas and are interpreted with regard to the plate tectonic setting of the Rwenzori micro-plate.

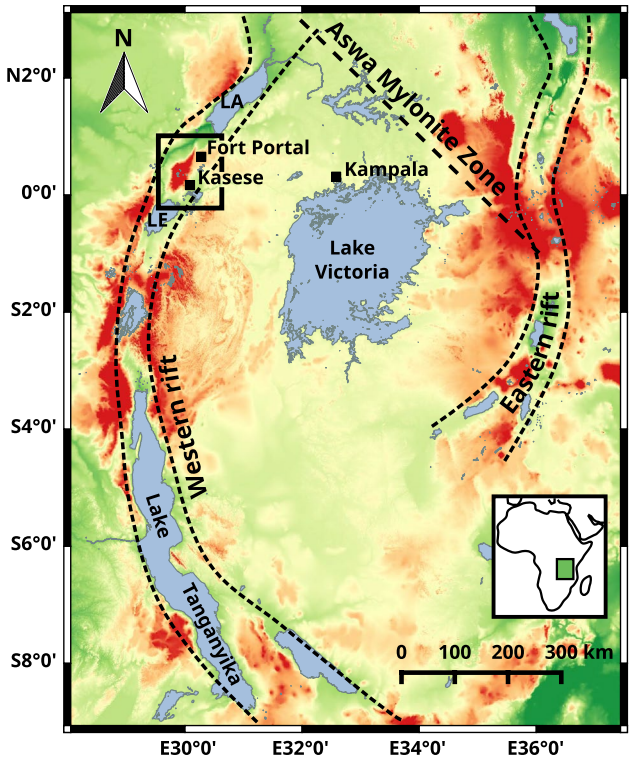

Fig. 1 Central part of the East African Rift System, which indicates important landmarks and outlines the main tectonic features. The *black frame* indicates the study area (see Fig. 2). *LA* Lake Albert, *LE* Lake Edward

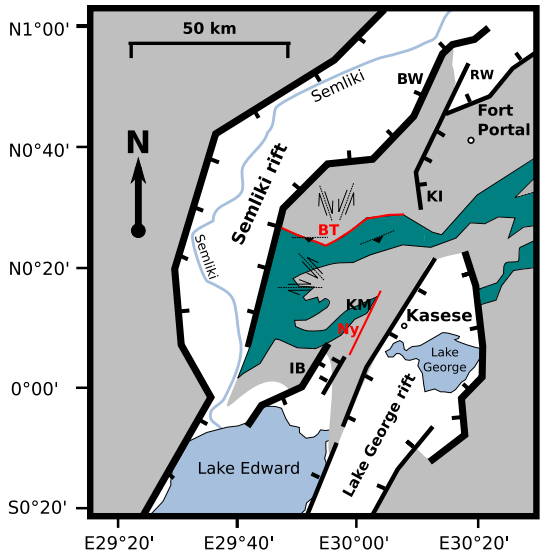

Fig. 2 Simplified geographical and geological overview map of the Rwenzori area (adapted from Link et al. 2010). *Gray units* represent gneisses of the Gneissic-Granulite Complex and sandstones, conglomerates, and argillaceous sediments of the Kibaran Belt. *Green units* represent the Buganda-Toro Belt, consisting mainly of schists, amphibolites, and quartzites. *Thick black lines* mark major boundary faults of the rifts and within the Rwenzori horst, *red lines* mark important ductile shear zones. *Thin dashed lines* indicate populations of small brittle faults. *BT* Buganda-Toro shear, *Bw* Bwamba fault, *Ny* Nyamwamba ductile shear zone, *IB* Ibimbo fault, *RW* Ruimi-Wasa fault, *KI* Kisomoro fault

Geology and kinematics of the Rwenzori Mountains

Geology and structure

The Rwenzori Mountains form a 100-km-long, 50-km-wide horst block, bounded by en echelon faults. The mountain range is situated within a rift-transfer zone, which connects two rift segments of the Albertine Rift. The Albertine Rift forms the northern part of the western branch of the EARS.

The northern Rwenzori area and the Rwenzori block itself are comprised of gneisses from the Archaean Gneissic-Granulite Complex that are inter-layered with meta-sediments (schist, amphibolites, and quartzites) associated with the paleo-proterozoic Buganda-Toro Belt (Fig. 2). In the southern Rwenzori region, also argillaceous sediments of the meso-proterozoic Kibaran Belt appear.

The Rwenzori block is bounded by a number of major border faults and fault networks, which separate it from the surrounding plates and rift grabens (Fig. 2). In the west, the block is bounded by the Bwamba normal fault, which dips toward the Semliki rift valley (Koehn et al. 2008). Along this line, the Rwenzori block is completely detached from the adjacent Congo craton.

The situation in the NE, where the Rwenzori block is bounded by the NNE striking Ruimi-Wasa fault, is slightly more complicated. In the very N, the Ruimi-Wasa fault borders against a fully developed rift basin and branches out with a NE striking major fault N of Fort Portal (see Fig. 2). In its central to northern central range (between c. N0°40′ and N0°20′), the Rwenzori block is still in contact with the Tanzania craton in its east (Fig. 2). Toward the central Rwenzoris, the Ruimi-Wasa fault is replaced by the NNW–SSE striking Kisomoro fault. Seismic fault plane solutions (Fig. 3, from Lindenfeld et al. 2012) indicate that the dominant displacement on the Kisomoro fault is normal. The S of the Rwenzori horst is segmented by several NE–SW striking large-scale normal faults.

Detailed structural mapping of mainly smaller brittle faults in the Rwenzori Mountains reveals complex fault systems in the central Rwenzoris (Koehn et al. 2008; Link et al. 2010). Polyphase stress fields induced brittle northward-directed thrusting and at least two minor strike slip events with roughly N–S and E–W compression and SW–NE striking normal faults (Sachau et al. 2011), visible as populations of smaller faults. Figure 2 includes a schematic overview of these fault systems. The data can be resolved into two small- to medium-scale fault populations: range-parallel faults that are oriented parallel to the main normal

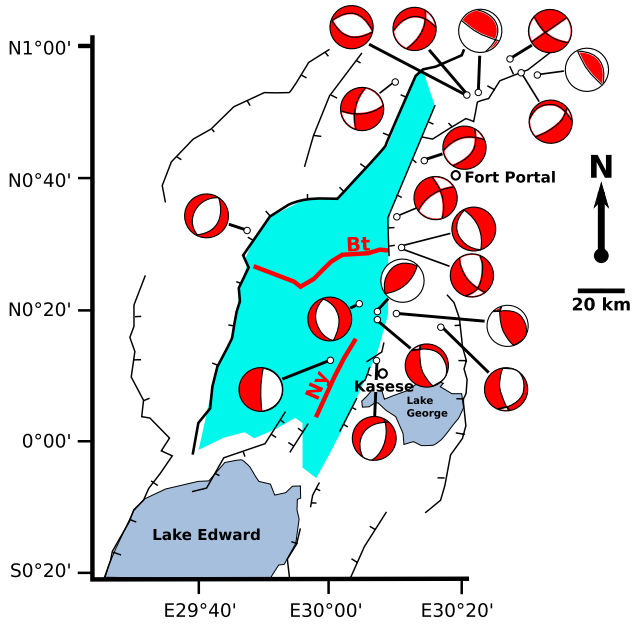

Fig. 3 Simplified tectonic map of the Rwenzori area with 19 fault plane solutions of seismic events (Lindenfeld et al. 2012) around the Rwenzori micro-plate. Fault plane solutions show compressional quadrants in *red* and extensional quadrants in *white*. *Black symbols* in the interior of the Rwenzoris mark the approx. location of the dominating brittle fault systems. The fault plane solutions illustrate the heterogeneity of the local present-day stress field. The Rwenzori Mountains are indicated by a *turquoise background color*

faults around the Rwenzori range and transsection faults cross-cutting the central Rwenzoris at various angles. It has been proposed that the center of the Rwenzoris has been also segmented by large-scale faults, similar to the situation in the S (Ring 2008).

Figure 3 displays major brittle structures in combination with a number of selected fault plane solutions of seismic events in the area, acquired by Lindenfeld et al. (2012). The displayed solutions indicate the large heterogeneity of the present-day stress field in the Rwenzori area, which is further discussed in later sections.

Pre-rift paleo-stresses and brittle structures in the Rwenzori area are not well known. The EARS in general has a polyphase brittle deformation history, and it can be assumed that this is true for the Rwenzori area as well. Older pre-rift brittle faults may be present in the Rwenzori Mountains. Delvaux et al. (2012) mention two brittle events in the Rukwa basin south of the Albertine rift, one event being compressional and the second event strike slip. Especially, the steep reverse faults in the center of the Rwenzori Mountains that indicate NNW-directed shorting may represent one of these pre-rift events.

Figure 4 shows typical faults from the area, which are typically either in metamorphic host rocks or in young, little consolidated sediments (here volcanic ash).

Cross-cutting relationships of faults in the Rwenzori Mountains are not always clear, so that it is not straightforward to produce detailed age relationships of faults. The best cross-cutting relationships are visible in the northern part of the Rwenzori Mountains where rift-related normal faulting is older than strike slip and oblique slip faulting. This relation can be seen in several locations in the north where shallow to horizontal striations and slicken-fibers overprint steep ones. The youngest faults in the NE corner of the northern part of the Rwenzori Mountains are steep reverse faults that either overprint strike slip faulting or is coeval to strike slip faulting. Age relationships of faults in the center of the Rwenzori Mountains are not clear; however, the displacement of tunnel walls cut by faults in the Kilembe mine indicates that oblique slip movements have been active within the last 30 years. One of these faults shows an estimated slip rate of 0.5 mm/year.

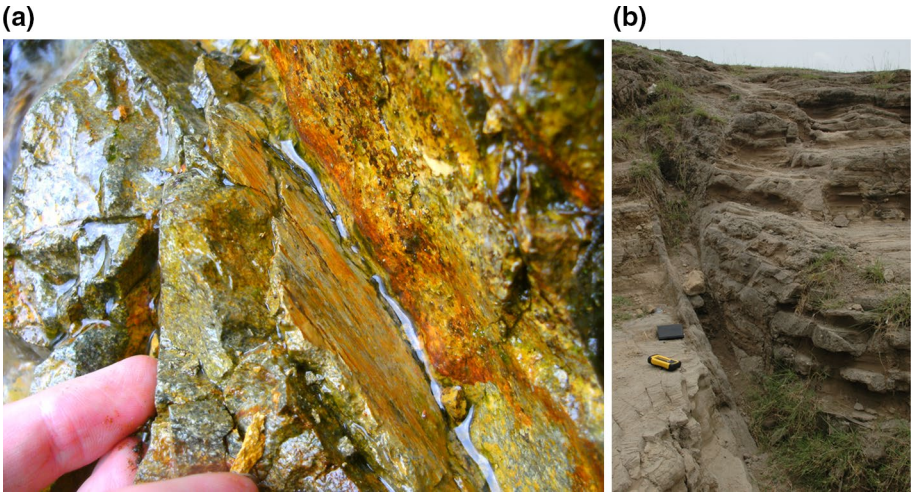

Fig. 4 Photographs of brittle faults typical for the Rwenzori area. **a** Fault plane with lineation in amphibolite in the central Rwenzoris. **b** Flower structure in young volcanic ash near Lake Edwards

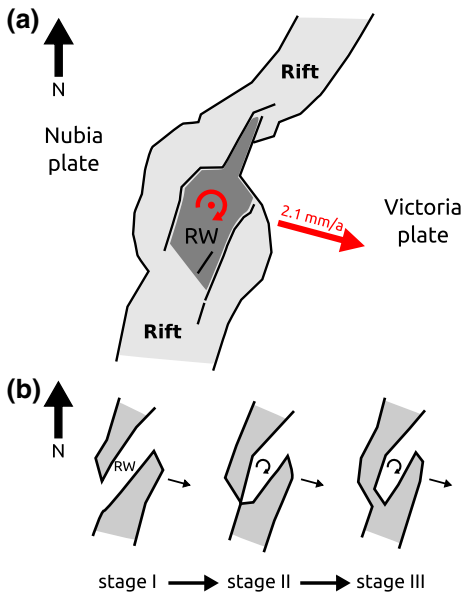

Fig. 5 **a** Plate movements of the Rwenzori micro-plate and the Victoria plate, with fixed Nubia plate. *Marked* is the proposed center of rotation of the Rwenzori block and the translation of the Victoria plate. **b** Proposed stages of the Rwenzori development (Koehn et al. 2008). *Stage I* initial development; *stage II* block rotation; *stage III* capturing and detachment

Active kinematics

The Albertine Rift System forms the northern part of the western branch of the East African Rift System (EARS) located between the Nubian plate to the west and the Victoria block to the east (Fig. 5a). The Victoria block encompasses the Tanzania craton and is bounded by Proterozoic mobile belts (i.e., Fernandes et al. 2013). The Nubian plate can be identified with the region west of the EARS following previously defined boundaries of the African plate (Horner-Johnson et al. 2005), including the Congo craton. Since the Rwenzori block itself is enclosed by major faults, we consider it a micro-plate. Here, we use the terms block and micro-plate a synonyms.

Geodetic studies indicate that the Victoria plate between the western and eastern rifts of the EARS rotates anticlockwise with respect to the Nubian plate with the Albertine rift opening with a velocity of approximately 2.1 mm per year in an ESE direction (e.g., Stamps et al. 2008; Fernandes et al. 2013; Saria et al. 2014). Structural and seismic data used to test numerical models indicate the Rwenzori block itself rotates clockwise (Koehn et al. 2010; Fig. 5a). These authors suggest that the Rwenzori block is detached from the neighboring plates in the south, but still attached to the Victoria block in the north. The Rwenzori block may be tilted along a NNE–SSW trending axis, with the highest peak to the west (Osmaston 1989; Taylor and Howard 1998); however, the southern third of the Rwenzori block does not seem to be affected by this tilt (Koehn et al. 2010; Bauer et al. 2013).

The western rift of the EARS is split into several 100- to 300-km-length segments (e.g., Morley and Nelson 1990; Ebinger 1989). These segments are initiated with the onset of sediment deposition from which rift propagation ensues.

The Rwenzori Mountains act as a rift-transfer zone at the intersection of two rift segments, the southern segment of the Albertine Rift System near Lake Edwards to the south of the Rwenzori Mountains and a segment to the north near Lake Albert. Koehn et al. (2008, 2010) suggest these segments migrated toward each other and captured the Rwenzori basement block (Fig. 5b). Block capturing of this type also occurs in other locations within the EARS such as the Mbeya Mountains in Tanzania and the Amaro Horst in Ethiopia (Bahat and Mohr 1987).

The southern western branch began opening 25 Mya (Roberts et al. 2012), but the timing of the northern western branch opening and capture of the Rwenzori block is still under debate. Previous research by Koehn et al. (2010), which is based on numerical models, suggests three main stages. Following Fig. 5b, Stage I began approximately 15 Ma and continued for about 2 Ma. During this stage, the rift segments to the north and south of the present-day Rwenzori Mountains were initiated. In Stage II, which lasted approximately 4 Ma, the two rift segments propagated toward each other. The Rwenzori block rotates clockwise, because it is still attached to the Nubia plate in the west and the Victoria plate in the north. In Stage III, which began 8–10 Ma ago, the present-day Rwenzori block forms and becomes detached from the adjacent plates except in the northeast, where it is still attached to the Victoria block and detachment is still ongoing.

Materials and methods

Stress inversion methods

Two different methods to calculate stress fields from fault-slip data have been applied in this work: the PBT method (Turner 1953) and the direct inversion method (Angelier 1990).

The PBT method is based on the Mohr–Coulomb fracture criterion and calculates stresses from the orientation of single fault planes, where P is the axis of contraction, T the extension axis, and B is the neutral axis in the fault plane. Most studies identify the P-axis with σ_1, B with σ_2 and T with σ_3 (Sippel et al. 2009). The angle of internal friction (θ) is assumed to equal 30° in this study, as recommended for most geological materials in the crust (Sippel et al. 2009). The PBT methods considers all faults as being

formed and moved by the same stress field and ignores possible fault reactivation, which is an important shortcoming if applied to heterogeneous stress fields.

The direct inversion method is based on the Wallace–Bott hypothesis, which assumes that slip occurs in the direction parallel to the resolved shear stress on the fault plane (Θ), which in turn is determined by the orientation of the traction vector σ_3. Once a stress tensor σ is assumed, a slip direction on a given fault plane can be calculated and a misfit angle with the observed slip direction can be determined. The state of stress of a homogeneous stress field is then calculated by a minimization routine of the misfit angle for a sufficient number of fault-slip data.

This study employs mainly the multiple inverse method (MIM), which is optimized for highly heterogeneous fault-slip data as found in the Rwenzori area. The multiple inversion method extends the scheme of the direct inversion method. MIM extracts subsets with k elements from a given set of fault-slip data and applies a classical direct stress inversion as described above to the given subsets. The so-called fault-combination number k is given by the user and is usually in the range between $k = 3$ and $k = 8$. The number of subsets is given by the binomial coefficient of k and the total number of fault-slip data. As a result, correct stress states are expected to get a large number of 'votes' from the stress inversion on the subsets.

When applying the multiple inverse method to a data set, we calculated the results for $k = 3$, $k = 4$, and $k = 5$ in order to test the stability of the clusters. The displayed MIM plots were calculated with $k = 5$, as recommended by the authors of the method (Yamaji 2000).

We used the software TectonicsFP (Reiter and Acs 2003) to perform PBT and DIM calculations. The multiple inverse method was applied using the *Multiple Inverse Method Software Package* (Otsubo and Yamaji 2006; Yamaji 2000).

It is preferable to restrict stress inversion methods to data sets of small-sized areas, preferably on the outcrop scale, but certainly not on the regional scale (Pollard et al. 1993; Homberg et al. 1996; Tikoff and Wojtal 1999).

Data acquisition and sample localities

The fault plane data and fault-slip data used in this study have been acquired during yearly field campaigns from 2007 to 2012 as part of the "RiftLink" project, which is funded by the German Research Foundation (DFG). Existing data sets of the central and northern Rwenzoris could be significantly improved and expanded during the last field campaign in 2012. Thanks to road construction works for the new tar road from Fort Portal to Bundibugyo, it was for the first time possible to acquire a significant number of fault-slip data from the NE.

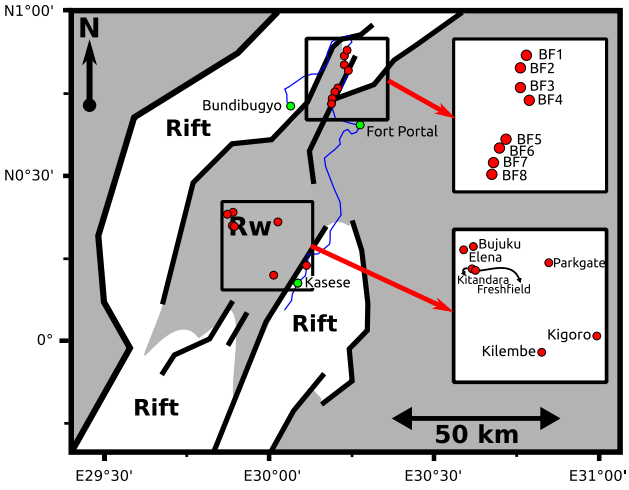

Fig. 6 Sample locations in the northern Rwenzoris and in the central Rwenzoris. *Red dots* are sample locations, and *green dots* are orientation points. These data come from two different domains, marked by the *rectangles*, which are referred to as the northern domain and the central domain in the text

For this study, we evaluated fault-slip data from a domain in the NE Rwenzoris, and from a domain in the central Rwenzoris (see Fig. 6 for sample localities). Two hundred and twenty-three fault plane orientations from the central part of the Rwenzoris and 120 fault planes from the very N of the Rwenzoris were used. Stress inversion at four localities in the very N is based on a total of 117 fault-slip data and on a total of 63 fault-slip data from three locations in the central Rwenzoris. Figure 7 gives an overview over the complete set of fault-slip data.

Individual data sets used for stress inversion consist of 18–43 fault-slip data, which we considered to be suitable for the applied stress inversion method (multiple inverse method, see below). The size of measured faults is typically on outcrop scale. Figure 5a shows a typical fault surface.

Each stress inversion was performed for the smallest possible area. In the N, the outcrop situation was partly good enough to collect sufficiently large fault-slip data sets for single outcrops. This was not possible in the high Rwenzoris, where the collected data represent localities in the immediate vicinity of Bujuku Hut, Kitandara Hut, and Elena Hut (Fig. 6).

Fault data from the northern domain have been acquired at eight different outcrops along an approximately N–S profile over a distance of 18 km, along the NE boundary of the Rwenzori block. The profile is of particular interest, because it covers a line from where the rift graben is already fully developed (location BF1 in Fig. 6) to a location where the Rwenzori block is still connected to the Victoria plate (location BF7/BF8 in Fig. 6).

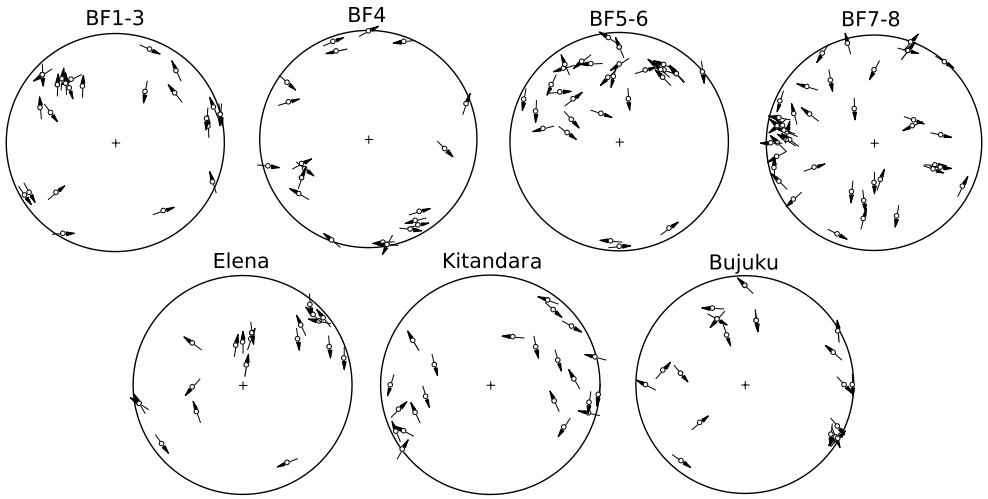

Fig. 7 Hoeppener plots of the fault-slip data, which are used for stress inversion. The localities are indicated according to Fig. 5. Fault planes are indicated by their corresponding poles in lower hemisphere projection. Fault plane lineations are drawn into the pole points. *Arrow heads* indicate the sense of movement of the hanging wall block

Results

In the following, we present structural data and the results of the stress inversion. In case of stress inversion, we display and interpret mainly results from the MIM method, which is best fitted to deal with the large heterogeneity of the fault-slip data in the Rwenzori area. The heterogeneity is both, spatial and temporal, meaning that variations of the recorded stress state occur between neighboring outcrops as well as in the fault-slip data of individual outcrops.

The large temporal variation of local stress fields, further discussed below, leads to frequent reactivation of existing fault planes, combined with the creation of new fault planes. In effect, the scatter in PBT results of large data sets is considerable and makes the detection of meaningful clusters highly speculative. Furthermore, slip indicators on fault surfaces are usually not genetically related to the fault plane, which distorts results from the PBT method even further.

A similar argument prevents an analysis of the data by direct inversion method, since the method yields meaningful results only if a set of at least four genetically related slip indicators is analyzed. The required genetic relation can usually not be guaranteed.

Presentation

PBT results are shown as plots of the kinematic axes for every fault datum of the data set in a lower hemisphere stereo net (Fig. 8). *P* is the axis of compression, *T* the axis of extension, and *B* the neutral axis. Occasionally, also the mean vectors and the associated cones of confidence with a significance of 99 % are given. Results of the direct inversion method are indicated by the principal stress axes plotted on a lower hemisphere stereogram (Fig. 8).

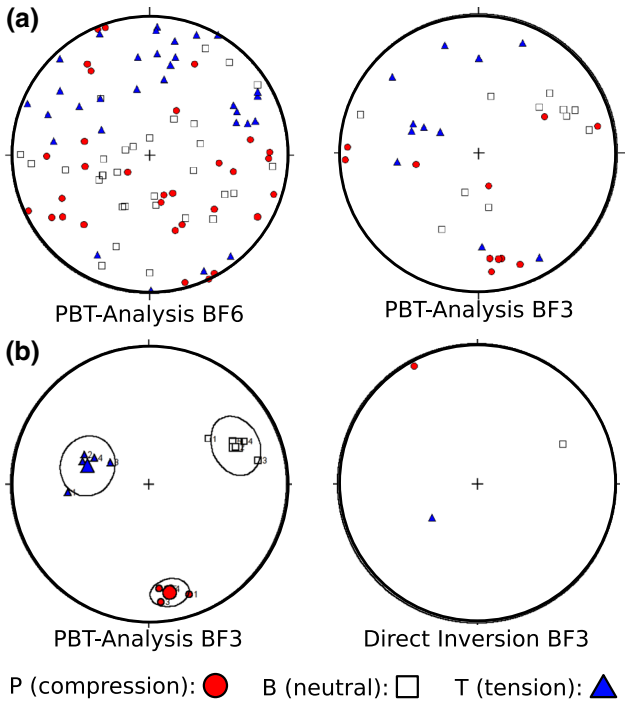

Fig. 8 Stress inversion results visualizing the heterogeneity and the rotation of the recorded stress field. **a** Stereoplots display results of the PBT method, which calculates stress from the orientation of single fault planes, for outcrops BF6 and BF3 in the northern Rwenzoris. The BF6 data are more heterogeneous than BF3, which is the least heterogeneous data set in this study. **b** Stereoplot of a homogeneous subset in the BF3 data. The results from PBT and the results from DIM differ by 30°, both with very small error margins. See text for further explanation

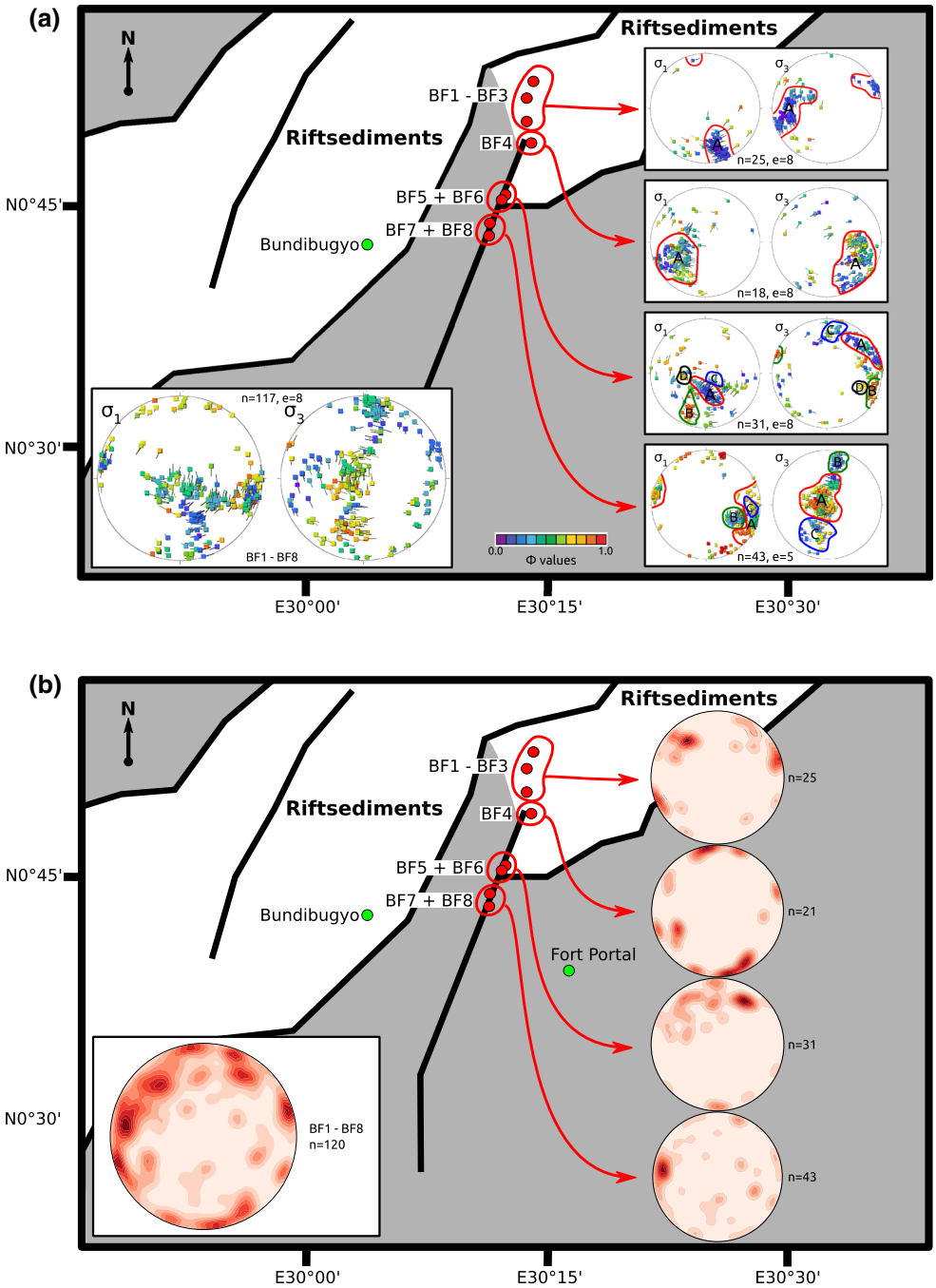

Fig. 9 Results of the MIM calculations and fault plane distribution for data from the northern domain, shown in lower hemisphere stereoplots. *Green dots* landmarks, *red dots* sample locations. **a** Results of MIM calculations for data sets from individual outcrops or combinations of adjacent outcrops. *Bottom left* is a plot of MIM results for the combined data set of all outcrops. *Colors* indicate Φ values, *violet* and *red* are uniaxial states of stress. **b** Contour plots of poles to fault planes, for the same data sets as in **a**

Results of the multiple inverse method are shown as poles of the principal stress axes σ_1 and σ_3, plotted to separate lower hemisphere stereograms. Colors indicate the value of the stress ratio $\Phi = (\sigma_2 - \sigma_3)/(\sigma_1 - \sigma_3)$ (Figs. 9a, 10a) σ_1, which is an useful indicator for the state of stress (Yamaji 2000). $\Phi = 0$ and $\Phi = 1$ indicate an axial state of stress, with $\sigma_1 > \sigma_2 = \sigma_3$ or $\sigma_1 = \sigma_2 > \sigma_3$, respectively. A triaxial state of stress is indicated if $0 < \Phi < 1$. Steep (inclination of $> 45°$) σ_1 or σ_3 axes indicate normal or reverse faulting, respectively, while a steep σ_2 axis is a sign for strike slip faulting.

Statistical fault plane data are shown in lower hemisphere stereo plots, displaying the contoured lower

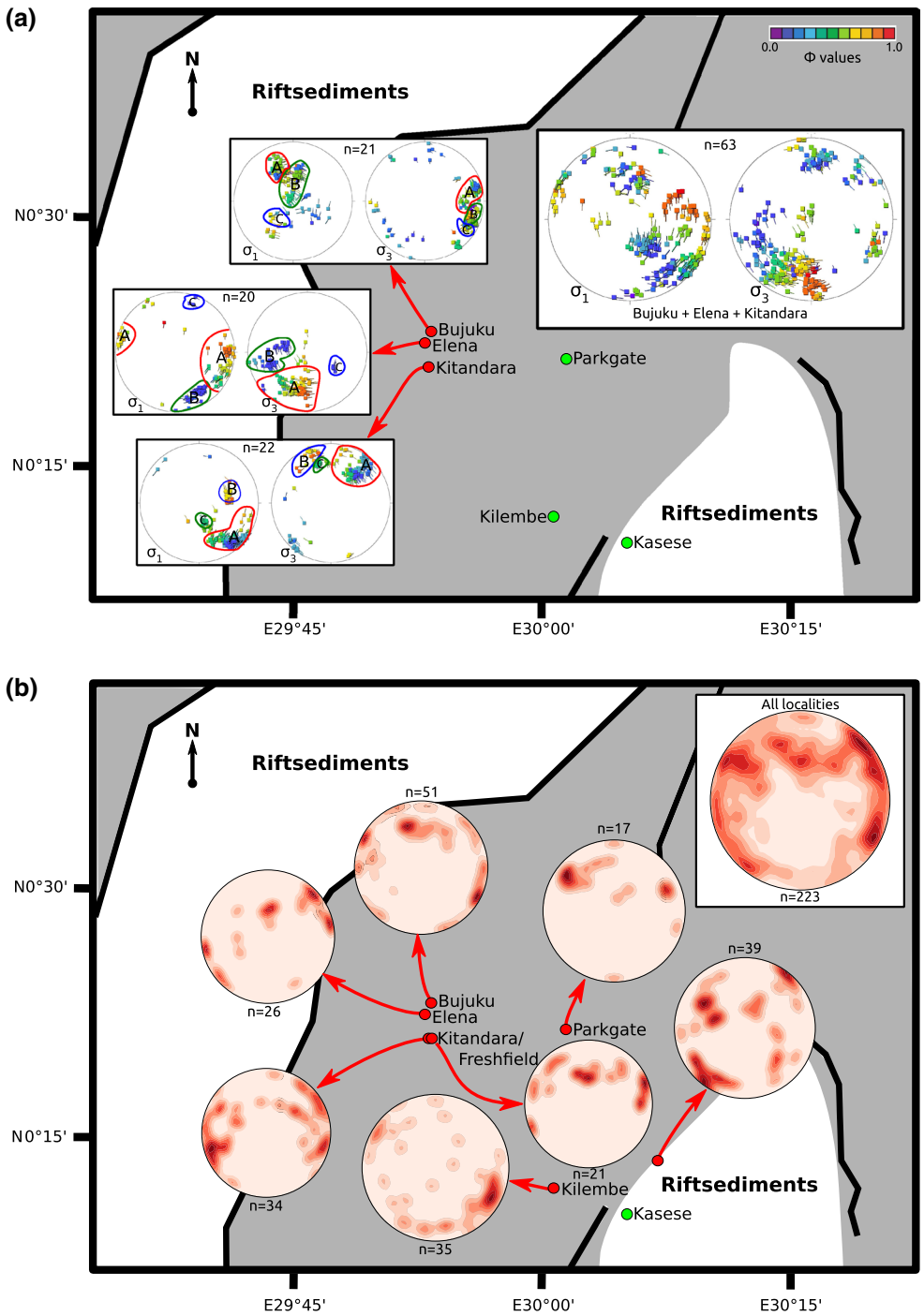

Fig. 10 Results of the MIM calculations and fault plane distribution for data from the central and the eastern Rwenzoris, shown in lower hemisphere stereoplots. The further description is identical to Fig. 8

hemisphere projection of the poles to the fault planes (Figs. 9b, 10b). MIM results and fault plane distributions are displayed for each individual locality and fault-slip data covering the entire northern and central domain.

General stress field and fault population

Figures 9a and 10a show the results of the multiple inverse method applied to the complete fault-slip data in the respective domains. Figures 9b and 10b display plots of the

general trend of the fault populations in the northern and in the central domain.

The northern domain is dominated by steep dipping fault planes. Three dominant subsets exist, striking approximate NE–SW, E–W, and NNW–SSE. The dip varies typically between 90° and 70°, which is consistent with both, normal and strike slip faulting conditions at the time, when the fault planes where initiated. A plot of the MIM results for the complete data set from the N displays three dominant clusters. These clusters indicate two N–S-directed tensile events with normal slip conditions and a different event with E–W-directed reverse slip, indicating E–W compression (Fig. 9a).

The variability of recorded stress fields is less pronounced in the central Rwenzoris, compared with the N. Despite the signs for multiple distinct events, only two clearly defined states of stress exist. One dominant event consists of a N–S-directed extension under normal slip conditions, and other events show roughly NE–SW-directed extension combined with SE–NW-directed compression, indicating strike slip to reverse slip conditions.

Temporal variation of stress inversion results

The heterogeneity of the fault population from single outcrop locations is exemplary demonstrated in Fig. 8a, where a lower hemisphere plot of *P*-, *B*-, and *T*-axes derived from the planes of the fault population at outcrop BF6 in the N domain is shown. It is evident, that any attempt to determine clusters can be speculative at best. This is a clear sign that stress field rotation occurred syn-tectonically, resulting in a broad scatter of the results.

The degree by which local outcrops have been affected by stress field rotation can be demonstrated if the results of the PBT method are directly compared to results of the DI Method, given that a subgroup of the recorded fault planes and fault lineations mirror distinct singular, but different events. This was possible in case of a subset of the fault-slip data from location BF3 (PBT results of the total fault population is shown in Fig. 8a, right, and results of the subset in Fig. 8b, left). Results of the direct inversion method, applied to the same subset, are shown in Fig. 8b, right.

A comparison of the mean vectors from the PBT analysis with the principal stress resulting from the direct inversion method yields the angular distance Θ. For the angle between the *P*-axis and the σ_1-axis results, $\Theta = 31°$, and for the *T*-axis and the σ_3-axis results, $\Theta = 32°$. The deviation of single results from the mean vector of the *P*-, *B*- and *T*-axes is between 1 and 4 %, and the deviation in case of the DI method is 3° at maximum.

This rotation of more than 30° indicates the presence of at least two independent events, where the later one reactivated and overprinted existing fault planes. While the stress derived from fault plane orientation indicates normal faulting and tensile conditions, the later event, derived from the lineation, indicates reverse faulting and compression.

Spatial variation of stress inversion results

Stress fields calculated from fault-slip data of the northern domain are significantly different from those calculated from stress inversion results of the central domain. The spatial heterogeneity of calculated stress poles is larger in the northern Rwenzoris, compared with the central Rwenzoris (compare Figs. 9, 10). Also the orientation of fault planes differs significantly between individual outcrops in the northern domain (Figs. 9b, 10b), more so than in the center. For this reason, results for the northern and for the central domain are presented separately.

Northern domain

Figure 9a displays the results of the multiple inverse method for different locations in the N. Strong variations in the stress inversion results indicate the variability of local stress fields, both temporal and spatial. No distinct first-order signals, caused by the continental extension, dominate the stress inversion results in the sense of a single repeating signal, which occurs over all domains.

Two possible exceptions from this rule are cluster A at localities BF1–BF3, which is similar to cluster A at locality BF5–BF6, and cluster A at locality BF4, which resembles cluster B at locality BF5. These clusters indicate ENE–WSW and ESE–WNW extension, respectively, for outcrops BF1 to BF4, located in the N. The extent of the clusters indicates a transition of the general stress state between normal faulting and strike slip faulting.

It is, however, possible to identify a general trend in the local stress inversion results. This trend indicates a transition of the stress regime from the northernmost outcrops, where a rift graben has been formed, to the localities further south, where the Rwenzori block is still attached to the Victoria plate.

Strike and dip of fault planes (Fig. 9b) varies significantly between the localities, just as the results of the stress inversion. The stress inversion results are usually not compatible with the fault plane orientation, which indicates a major reactivation of existing planes including inversion of the stress field. This is consistent with field observations of reverse slip indicators. The general orientation of fault planes is indicated by a dominance of N–S to NNE–SSW striking fault planes with steep to intermediate dip to the E.

The orientation of the σ_1 poles at outcrops in the very S of the northern domain, at locations BF7 and BF8, indicates ESE–WNW compression. Tensile polyphase stress is oriented at NNE–SSW and vertical, respectively. Thus, the

general stress state varies between strike slip and compressive reverse faulting conditions.

Outcrops BF5 and BF6 are located at the intersection of the main boundary faults in the NE and mark the transition between the stress regimes in the S and the N of the profile. The tensile stress in these outcrops spans the whole range from ESE–WSW to N–S tension. This orientation of the tensile stress is consistent with the adjacent main boundary normal faults, whose sense of displacement is indicated by recent seismic data (Koehn et al. 2010) and the general presence of a graben.

Figure 9 includes MIM results based on the entire data set from the N, using the complete data set of outcrops BF1 to BF8. This larger data set can help to identify the most dominant recorded stress fields for the whole area, instead of just single outcrops. Here, the clearest signals indicate two NNE–SSW-directed tensile events with normal faulting (indicating vertical orientation of the maximum principal stress σ_1) and an event with ESE–WNW-directed compression and reverse faulting (vertical σ_3-orientation).

Central Rwenzoris

Multiple inverse method (MIM) stereo plots based on fault-slip data from Kitandara Hut and from Elena Hut are very similar, with three dominant events indicating approximate SE–NW compression and N–S to SW–NE extension. These events also show similar stress ratios (Fig. 10a). A stereoplot of MIM (Fig. 10a) generated stress poles from Bujuku Hut displays a very different stress scenario, with three dominant events with ESE–WNW extension associated with normal fault conditions.

The stress poles calculated for Elena Hut and for the entire data set from Elena, Bujuku, and Kitandara indicate also minor reverse tectonics, with vertical σ_3 and compression with either N–S or NW–SE orientation (Fig. 10a).

All locations in the central Rwenzoris show two dominant fault populations: a set of normal fault planes combined with a set of steeply dipping fault planes indicating strike slip. Planes to normal faults strike usually approximately NE–SW, and slip indicators on these normal faults indicate late reverse slip.

The other dominant elements in the central Rwenzoris are steep fault planes, indicating strike slip faulting, typically striking approximate NW–SE. The exceptions are the surroundings of Bujuku hut, where steep fault planes strike in a NE–SW direction.

Discussion

Brittle faulting in the area may have started as early as the early Phanerozoic, when the Precambrian rocks in the Rwenzori area were exhumed above the 300 °C isotherm (Bauer et al. 2010), but fault slip caused by recent Cenozoic rifting of the Nubia–Somalia plate boundary overprints existing structures. This assumption is supported by the typical mismatch between the stress indicated by the orientation of fault planes and stress calculated from slip indicators on the fault planes. Heterogeneity of calculated stresses, both in space and time, hint at crustal deformation associated with rifting and block capture that is consistent with numerical modeling of these processes (Koehn et al. 2010). Associated syn-tectonic changes of local stress fields are also consistent with this hypothesis as shown by Sachau et al. (2011) in a numerical model.

The variation in local stress fields detected in this work may be related to crustal deformation from past, present, or overprinting of present-day tectonics on existing structures (Corti et al. 2011). Kinematic movements possibly affecting the local stress fields include (1) rotation of the first-order stress field, (2) new border fault creation to the NE and east of the Rwenzori, (3) active rotation of the Rwenzori micro-plate relative to the diverging Nubian and Victoria plates, or (4) rotation of internal blocks from segmentation of the Rwenzoris.

1. The amount of rotation of the first-order stress field in the western branch of the EARS is still under debate. However, stress reorientation at the order of up to $7.5°/10^5$ years has been suggested for East Africa (Bosworth et al. 1992) and may have occurred in this region. Stress reorientation acting on or creating the complex geometry of the rift in the northwestern Rwenzori region could explain strong heterogeneities in the local stress field there. In this region, two major rift faults with different strike intersect (Figs. 2, 3, 4). The major border fault strikes NNE–SSW dipping ESE, while the other major fault strikes ENE–WSE dipping to the N.
2. Active rifts that overprint existing heterogeneities can develop new border faults along zones of weakness (Van Wijk and Blackman 2005). New seismic studies suggest regions of melt intrusions in the crust east of the Rwenzori and north of the Rwenzori (Lindenfeld et al. 2012) where we find significant variations in the local stress field. Active magmatism can weaken the lithosphere (Buck 2006) allowing for rupture to occur in regions without large boundary forces, i.e., from subduction, such that new faults will develop. The complex local stress field in the NE of the Rwenzori is consistent with new border fault creation here such that the horst will become detached from the Victoria block.
3. The strong variability of the stress field in the northern Rwenzoris and relatively less heterogeneous stress fields in the central Rwenzoris can be explained by

rotation of the Rwenzori block with respect to the Nubian and Victoria plates. The anticlockwise rotation of the Victoria plate with respect to the Nubian plate results in transtension relative to the Rwenzori micro-plate, which may be exacerbated if the Rwenzoris are actively rotating clockwise. Transtension, which includes both normal slip and strike slip events, can explain the wide scatter of stress poles in the stereoplot for individual events. Even clusters, which can be attributed to single events [for instance at locality BF1 (Fig. 9a)], span typically the whole range of stress fields, where either σ_1, σ_2, or σ_3 form the vertical principal normal stress component. This results in either strike slip, normal slip, or reverse slip. Outcrops with clearly distinguishable events show the same pattern of alternating pure shear and simple shear conditions (outcrops BF5 to BF8 in Fig. 9a).

The dominance of generally steep fault planes in the N can be explained by oblique divergence of the Nubian and Victoria plate. Present-day steep faults accommodated shear in the past, before the onset of normal and reverse slip. Thus several faulting events are overprinted by present-day slip indicators. The large number of individual events found in our stress inversions is indicative of strain partitioning, where two different stress regimes have to be accommodated.

In the southern localities of the northern domain, where the Rwenzori block is still attached to the Victoria plate, fault inversion with local horizontal shortening occurs. This can be explained by rotation of the Rwenzori block relative to the surrounding plates such that compression occurs in the NE. Localities at more northward positions, where the Rwenzori plate is already detached from the Victoria plate and a rift graben has formed, do not show any signs of a major compression. This may suggest that compression occurred only after the rift formation.

Recent seismic data (Lindenfeld et al. 2012) have shown that the sense of the major fault in vicinity of the outcrop locations in the N is presently normal with a sinistral component. This indicates approximately ESE tension, parallel to the general translation vector of the Victoria plate.

The spatial variation of calculated stress poles is less pronounced in the central Rwenzori when compared to the north (Figs. 9a, 10a). This is not surprising, since the area is located in the interior of the Rwenzori micro-plate suggesting that the central Rwenzoris are not affected by plate–plate interactions.

4. It has been proposed that the central Rwenzoris have been segmented into internal blocks by transsection faults, each with its own kinematics and its own local stress field (e.g., Ring 2008; Bauer et al. 2013). The lineament map (Fig. 11) suggests that the sample localities at Kitandara and Elena Hut are on the same block, while Bujuku is on a different block. A multiple block model can explain that the calculated stress field for Elena and Bujuku are distinctly different despite their geographical proximity. The same argument applies the similarity of calculated stress poles for data from Elena and Kitandara; however, it is difficult to distinguish between present-day and paleo-stress fields in the central Rwenzori where geodetic observations of surface motions are needed to test an actively segmenting Rwenzori block model.

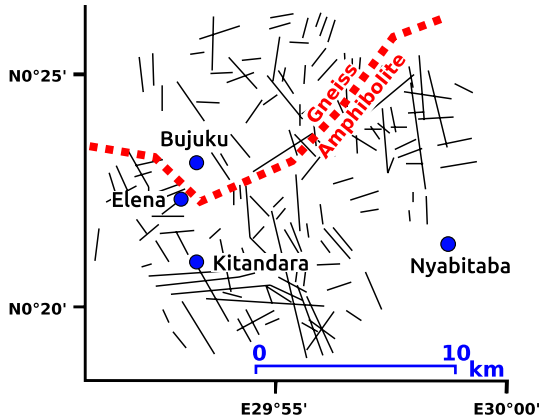

Fig. 11 Lineament map of the central Rwenzoris. Lineaments are linear features in the landscape

Conclusion

Fault-slip data from the northern Rwenzori show an unusually large heterogeneity, both in space and time, compared with other studies applying stress inversion. Individual localities in the northern domain experience polyphase tectonics, probably due to transpression tectonics of the Victoria plate and the Rwenzori micro-plate. Each phase of tectonic stress affects the local fault population, leading to heterogeneous fault-slip data. Faults show strong overprinting relationships and the stress field that initiated the fault plane is usually not the same that created the slip indicators.

Fault-slip data from the central Rwenzori are more homogeneous compared wtih stress fields along the borders of the micro-plate. The results of the fault inversion in that domain, in conjunction with the visible lineaments, may indicate independent stress fields for multiple blocks in the central Rwenzori area.

Acknowledgments We acknowledge funding by the Deutsche Forschungsgemeinschaft (DFG), Grant KO 2463/4-2. D. S. Stamps is funded by the NSF EAR Postdoctoral Fellowship program Grant #EAR1249295.

References

Angelier J (1990) Inversion of field data in fault tectonics to obtain the regional stress—III. A new rapid direct inversion method by analytical means. Geophys J Int 103:363–376

Bahat D, Mohr P (1987) Horst faulting in continental rifts. Tectonophysics 141(1–3):61–73. doi:10.1016/0040-1951(87)90174-0

Bauer FU, Glasmacher UA, Ring U, Schumann A, Nagudi B (2010) Thermal and exhumation history of the central Rwenzori Mountains, Western Rift of the East African Rift System, Uganda. Int J Earth Sci 99:1575–1597

Bauer FU, Glasmacher UA, Ring U, Karl M, Schumann A, Nagudi B (2013) Tracing the exhumation history of the Rwenzori Mountains, Albertine Rift, Uganda, using low-temperature thermochronology. Tectonophysics 599:8–28. doi:10.1016/j.tecto.2013.03.032

Bosworth W (1985) Geometry of propagating continental rifts. Nature 316:625–627

Bosworth W, Strecker MR, Blisniuk PM (1992) Integration of East African paleostress and present-day stress data: implications for continental stress field dynamics. J Geophys Res 97(B8):11851. doi:10.1029/90JB02568

Buck WR (2006) The role of magma in the development of the Afro-Arabian rift system. In: Yirgu G, Ebinger CJ, Maguire PKH (eds) The afar volcanic province within the East African rift system. Geological Society Special Publications, London, pp 43–54

Calais E, Hartnady C, Ebinger C, Nocquet JM (2006) Kinematics of the East African Rift from GPS and earthquake slip vector data". In: Yirgu G, Ebinger CJ, Maguire PKH (eds) Structure and evolution of the rift systems within the Afar volcanic province, Northeast Africa, vol 259. Geological Society Special Publications, London, pp 9–22

Corti G, Calignano E, Petit C, Sani F (2011) Controls of lithospheric structure and plate kinematics on rift architecture and evolution: an experimental modeling of the Baikal rift. Tectonics 30(3):TC3011. doi:10.1029/2011TC002871

Delvaux D, Barth A (2010) African stress pattern from formal inversion of focal mechanism data. Tectonophysics 482:105–128

Delvaux D, Kervyn A, Macheyeki AS, Temu EB (2012) Geodynamic significance of the TRM segment in the East African Rift (W-Tanzania): active tectonics and paleostress in the Ufipa plateau and Rukwa basin. J Struct Geol 37:161–180

Ebinger CJ (1989) Tectonic development of the western branch of the East African rift system. Geol Soc Am Bull 101:885–903

Fernandes RMS, Miranda JM, Delvaux D, Stamps DS, Saria E (2013) Re-evaluation of the kinematics of Victoria Block using continuous GNSS data. Geophys J Int 193:1–10. doi:10.1093/gji/ggs071

Foster A, Francis N (1996) Comparisons between the rift systems of East Africa, Earth and Beta Regio, Venus. Earth Planet Sci Lett 143(1–4):183–195. doi:10.1016/0012-821X(96)00146-X

Homberg C, Hu JC, Angelier J, Bergerat F, Lacombe O (1996) Characterization of stress perturbations near major fault zones: insights from 2-D distinct-element numerical modelling and field studies (Jura Mountains). J Struct Geol 19:703–718

Horner-Johnson BC, Gordon RG, Cowles SM, Argus DF (2005) The angular velocity of Nubia relative to Somalia and the location of the Nubia–Somalia–Antarctica triple junction. Geophys J Int 162:221–238

Koehn D, Aanyu K, Haines S, Sachau T (2008) Rift nucleation, rift propagation and the creation of basement micro-plates within active rifts. Tectonophysics 458(1–4):105–116. doi:10.1016/j.tecto.2007.10.003

Koehn D, Lindenfeld M, Rümpker G, Aanyu K, Haines S, Passchier CW, Sachau T (2010) Active transsection faults in rift transfer zones: evidence for complex stress fields and implications for crustal fragmentation processes in the western branch of the East African rift. Int J Earth Sci 99(7):1633–1642. doi:10.1007/s00531-010-0525-2

Lindenfeld M, Rümpker G, Batte A, Schumann A (2012) Seismicity from February 2006 to September 2007 at the Rwenzori Mountains, East African Rift: earthquake distribution, magnitudes and source mechanisms. Solid Earth Discuss 4(1):251–264

Link K, Koehn D, Barth M, Tiberindwa J, Barifaijo E, Aanyu K, Foley S (2010) Continuous cratonic crust between the Congo and Tanzania blocks in western Uganda. Int J Earth Sci 99(7):1559–1573. doi:10.1007/s00531-010-0548-8

Macdonald KC, Scheirer DS, Carbotte SM (1991) Mid-ocean ridges: discontinuities, segments and giant cracks. Science 253(5023):986–994. doi:10.1126/science.253.5023.986

Morley CK, Nelson RA (1990) Transfer zones in the East African rift system and their relevance to hydrocarbon exploration in rifts (1). AAPG Bull 74:1234–1253

Moustafa AR (1997) Controls on the development and evolution of transfer zones: the influence of basement structure and sedimentary thickness in the Suez Rift and Red Sea. J Struct Geol 19(6):755–768. doi:10.1016/S0191-8141(97)00007-2

Osmaston H (1989) Glaciers, glaciations and equilibrium line altitudes on the Rwenzori. In: Mahaney WG (ed) Quaternary and environmental research on East African Mountains. Balkema, Rotterdam, pp 31–104

Otsubo M, Yamaji A (2006) Improved resolution of the multiple inverse method by eliminating erroneous solutions. Comput Geosci 32(8):1221–1227. doi:10.1016/j.cageo.2005.10.022

Pollard DD, Saltzer SD, Rubin AM (1993) Stress inversion methods: Are they based on faulty assumptions? J Struct Geol 1 15:1045–1054

Reiter F, Acs P (2003) TectonicsFP—a computer program for structural geology. http://www.tectonicsfp.com/

Ring U (2008) Extreme uplift of the Rwenzori Mountains in the East African Rift, Uganda: structural framework and possible role of glaciations. Tectonics 27(4):TC4018. doi:10.1029/2007TC002176

Roberts EM, Stevens NJ, O'Connor PM (2012) Initiation of the western branch of the East African Rift coeval with the eastern branch. Nat Geosci 5:289–294

Sachau T, Koehn D, Passchier C (2011) Lattice-particle simulation of stress patterns in a Rwenzori-type rift transfer zone. J Afr Earth Sci 61(4):286–295. doi:10.1016/j.jafrearsci.2011.08.006

Saria E, Calais E, Stamps DS, Delvaux D, Hartnady CJH (2014) Present-day kinematics of the East African Rift. J Geophys Res 119:3584–3600. doi:10.1002/2013JB010901

Shan Y, Li Z, Lin G (2004) A stress inversion procedure for automatic recognition of polyphase fault/slip data sets. J Struct Geol 26(5):919–925. doi:10.1016/j.jsg.2003.10.001

Sippel J, Scheck-Wenderoth M, Reicherter K, Mazur S (2009) Paleostress states at the South-Western margin of the Central European Basin System—application of fault-slip analysis to unravel a polyphase deformation pattern. Tectonophysics 470(1–2):129–146. doi:10.1016/j.tecto.2008.04.010

Stamps DS, Calais E, Saria E, Hartnady C, Nocquet J-M, Ebinger CJ, Fernandes RM (2008) A kinematic model for the East African Rift. Geophys Res Lett 35:L05304. doi:10.1029/2007GL032781

Taylor RG, Howard KWF (1998) Post-palaeozoic evolution of weathered land surfaces in Uganda by tectonically controlled cycles of deep weathering and stripping. Geomorphology 25:173–192

Tikoff B, Wojtal SF (1999) Displacement control of geologic structures. J Struct Geol 21:959–967

Turner FJ (1953) Nature and dynamic interpretation of deformation lamellae in calcite of three marbles. Am J Sci 251(4):276–298

Van Wijk JW, Blackman DK (2005) Dynamics of continental rift propagation: the end-member modes. Earth Planet Sci Lett 229:247–258

Yamaji A (2000) Multiple inverse method: a new technique to separate stresses from heterogeneous fault-slip data. J Struct Geol 22:441–452